

## Micromechanism for Metallic-Glass Formation by Solid-State Reactions

H. Schröder and K. Samwer

*I. Physikalisches Institut, Universität Göttingen, D-3400 Göttingen, Federal Republic of Germany*

and

U. Köster

*Abteilung Chemietechnik, Universität Dortmund, D-4600 Dortmund, Federal Republic of Germany*

(Received 7 November 1984)

Metallic-glass formation by solid-state reactions has been observed in multilayer Zr-Co diffusion couples and studied by cross-sectional transmission electron microscopy. Planar growth of a Co-rich amorphous phase proceeds from each interface of the unreacted sample, thus consuming the Co layers at a higher rate. Further annealing results eventually in a reaction of the Co-rich glassy phase with remaining Zr. Because of the high diffusivity of the Co in the amorphous phase, Kirkendall voids are formed during this homogenizing process and are lined up with the periodicity of the original layered structure.

PACS numbers: 61.40.Df, 61.55.Hg, 66.30.Fq, 82.20.Pm

A number of amorphous metals can be obtained by solid-state reactions without any rapid quenching of the alloy from either the melt or the vapor: In a first set of experiments amorphous metallic alloys were obtained by diffusion of Ag or Rh atoms into an already amorphous film of tellurium<sup>1</sup> or silicon,<sup>2,3</sup> respectively. Then, the crystalline intermetallic compound Zr<sub>3</sub>Rh was reported to transform at about 500 K by reaction with hydrogen into an amorphous metallic hydride<sup>4,5</sup>; since the diffusion of hydrogen at this relatively low temperature is still very high compared to the metal diffusion, the reaction is assumed to be controlled by the transformation of the crystalline compound into the amorphous metallic hydride at the interface. The amorphization can only occur because at the reaction temperature the time necessary for nucleation and growth of the stable crystalline phases is much larger.

Metallic-glass formation through solid-state interdiffusion in a multilayer structure of two crystalline metals was reported for the first time by Johnson and co-workers<sup>6-8</sup>; this reaction is assumed to be driven by the large negative heat of mixing of the two components and can proceed in a broad concentration range as long as the annealing temperature is high enough to allow sufficiently rapid interdiffusion of the metal atoms, but low enough to avoid any nucleation of the crystalline intermetallic compounds during the reaction time. In this case interdiffusion through the growing amorphous layer is assumed to be the dominating rate-limiting factor for the solid-state amorphization. Recent Rutherford backscattering data on the Hf-Ni reaction couple showed considerable deviations from the  $\sqrt{t}$  growth law<sup>9</sup> for short reaction times, but quite good agreement for longer annealing times.<sup>10</sup>

So far no direct information on the micromechanisms involved in solid-state amorphization is available, since neither Rutherford backscattering nor x-ray

diffraction provides any local structural information; both techniques probe only microscopically large areas. Cross-sectional transmission electron microscopy (TEM),<sup>11</sup> on the other hand, is known to be an extremely accurate technique for following growth kinetics as well as for analyzing micromechanisms in thin-film systems with well-defined layered structures. In this Letter we present for the first time results of a cross-sectional TEM analysis of the reaction in Zr-Co multilayer diffusion couples which enable us to propose a model for the solid-state amorphization reaction.

Zr-Co multilayer diffusion couples were prepared in a UHV system with two rate-controlled *e*-beam guns evaporating alternating layers of zirconium and cobalt; the use of a mechanical chopper excluded any possibility of simultaneous deposition of both metals. For the TEM samples an oxidized silicon wafer was used as a substrate which was always kept below 273 K during the deposition process to avoid uncontrolled reactions. For the solid-state reaction the samples were annealed *in situ* in the UHV system at temperatures around 500 K for times up to 24 h. For longer reaction times the samples were taken out of the UHV system. Samples for cross-sectional transmission electron microscopy were prepared with a variation of the Sheng-Marcus method<sup>12</sup>: Two pieces of the silicon wafer were glued face to face into a slotted stainless steel rod which was inserted into a brass tube 3 mm in diameter. Slices were cut from the above mentioned assembly and mechanically thinned. For the final thinning a Technics MIM IV ion-beam mill was used operating at 6 kV. Any amorphization during the ion-beam milling either by ion-beam mixing or by solid-state reaction due to the heating up during the milling process could be excluded from the microstructure observed in the as-deposited specimen. Successfully milled specimens were analyzed with a Philips 301 transmission electron

microscope at 100 kV.

Figure 1 shows the x-ray diffraction patterns of three reacted Zr-Co multilayered diffusion couples with different overall compositions and of one of the control samples kept at room temperature. For the Co-20-nm-Zr-34-nm sample ( $Zr_{45}Co_{55}$ ) reacted *in situ* for 24 h at 473 K, the x-ray diffraction pattern exhibits the features of an almost single amorphous phase. The concentration of this glass is within the range of glass formation predicted from a calculated free-energy versus concentration diagram using Miedema's parameter as discussed elsewhere.<sup>13, 14</sup>

Cross-sectional transmission electron microscopy of an unreacted  $Zr_{47}Co_{53}$  sample reveals clearly resolved alternating polycrystalline layers of Zr and Co with thicknesses in good agreement with those calculated from the evaporation parameter. No amorphous phase has been detected at the interfaces; the grain size in both metals is below 10 nm. The electron diffraction pattern consists of the well-known lines for fcc Co and hcp Zr in agreement with x-ray diffraction.

More interesting are pictures of partially reacted samples as shown in Figs. 2(a) and (2b) (annealed *in situ* for 2 h at 483 K): On top of an amorphous

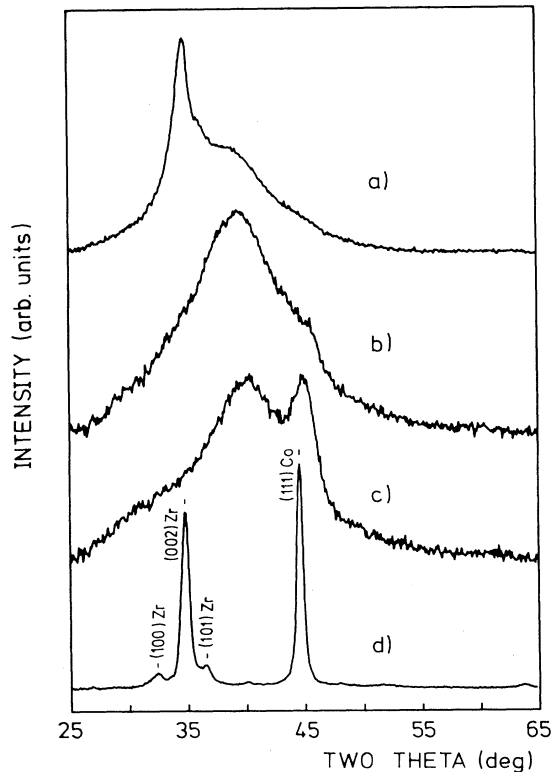


FIG. 1. X-ray diffraction pattern ( $Cu K\alpha$  radiation) vs scattering angle for four multilayer samples: (a)  $Zr_{50}Co_{50}$ ; (b)  $Zr_{45}Co_{55}$ ; (c)  $Zr_{40}Co_{60}$  (all reacted 24 h at 200°C *in situ*); (d)  $Zr_{40}Co_{60}$  (control film kept at room temperature).

$SiO_2$ -substrate layer a polycrystalline Zr layer can be revealed which was originally only half as thick as all the other Zr layers in order to symmetrize the diffusion process. After the mentioned annealing this layer is separated from the polycrystalline Co by an amorphous layer which exhibits the typical diffuse pattern of amorphous material due to the lack of long-range order. The following sequence of layers is indicated in Fig. 2(b) which demonstrates the strictness of the glass formation by the solid-state reaction. At each Zr-Co interface an amorphous layer is formed; all these layers show a uniform thickness and no signifi-

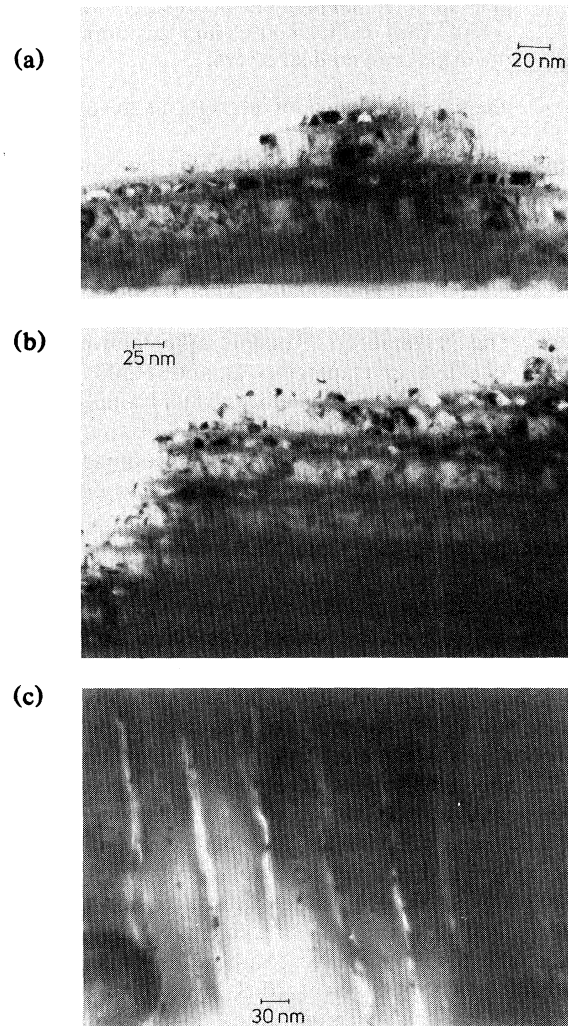


FIG. 2. (a) Cross-sectional TEM of a Zr-Co multilayer diffusion couple reacted 2 h at 210°C (see text for explanation). (b) Same as (a) on a smaller magnification: Note the strictness of the glass formation at each interface and its planar growth. (c) Cross-sectional TEM of a Zr-Co multilayer diffusion couple reacted over 100 h at 210°C. The reaction is almost complete with some remaining Zr crystals (black spots) and rows of Kirkendall voids.

cant deviation from a planar growth could be detected. It has to be mentioned that during this annealing for 2 h at 483 K in both metals grain growth proceeds up to a size comparable with the thickness of each layer. No Kirkendall voids are observed at this stage of the reaction.

Comparing the original thicknesses of the crystalline layers with the remaining ones shown in these micrographs, we observe a very asymmetric transformation rate, i.e., each amorphous layer consumed about twice as much Co as Zr. From this thickness relation one can calculate the average concentration of the amorphous layer to be about  $Zr_{20}Co_{80}$ .

Figure 2(c) shows a sample after annealing for over 100 h at 500 K which exhibits an almost complete amorphous microstructure with just a few small Zr crystals. These crystals are lined up indicating that they are not formed by crystallization of the already fully amorphized specimen, but are a remainder of the polycrystalline Zr layers. In this stage of the reaction a large number of Kirkendall voids are observed which form rows with the same periodicity as the original bilayer structure including the swelling of the material. Apart from one sharp ring which can be attributed to the Zr crystals the electron diffraction pattern consists of very broad rings. These rings are considerably broader than usually observed in liquid-quenched metallic glasses indicating a composition gradient in the amorphous phase.<sup>9</sup>

These results can be summarized in a schematic diagram (Fig. 3) of the micromechanisms which proceed during amorphization by solid-state reactions. Since

we observe the formation of amorphous layers of uniform thickness at each Zr-Co interface, nucleation of the amorphous phase is certainly very easy. We can conclude that the time necessary for nucleation is much smaller than for growth. Grain boundary triple points are known as preferred nucleation sites for heterogeneous nucleation of incoherent phases. The Co as well as the Zr layers consist of very small grains, thus exhibiting a large number of phase boundary triple points and therefore a very high density of nucleation sites for the amorphous phase. In recent experiments with thin Ni and Zr foils<sup>15,16</sup> grains are orders of magnitude larger than in our vapor-deposited films, but the cold working process necessary to reduce the thickness would produce a large number of defects and steps; such highly distorted interfaces might have already a structure similar to that of the amorphous phase.

As mentioned above, the growth of the amorphous layers is very asymmetrical leading to the formation of a Co-rich glass. Zr-Co glasses of about this composition are supposed to be the most stable, i.e., to be the glasses with the highest crystallization temperature. From a semiquantitative free-energy versus concentration diagram we know that an amorphous phase of such a composition can exist in a metastable equilibrium with pure crystalline Co. Obviously, it is easier for the system to achieve this metastable equilibrium than the other one between a more Zr-rich glass and pure crystalline Zr. Atomic jumps across the interface, which lower locally the free energy of the system, seem to be easier for the smaller Co atoms, thus estab-

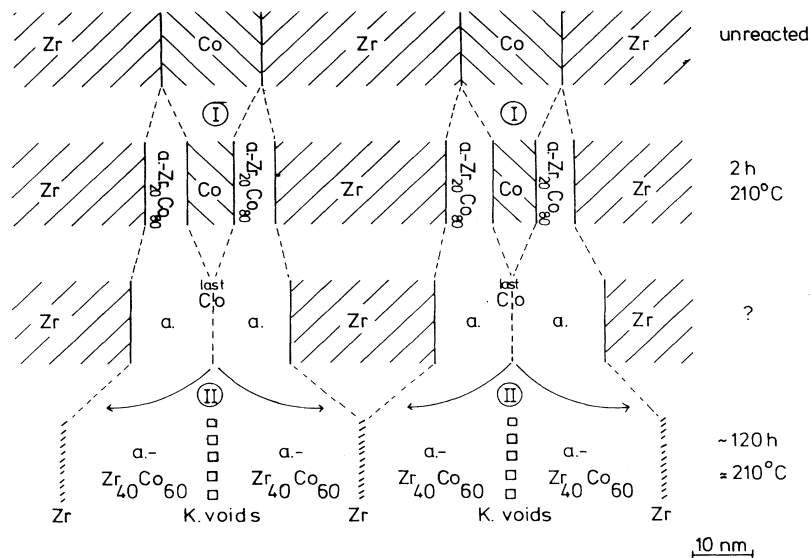


FIG. 3. Schematic diagram of the reaction process: Note the asymmetric (2:1) growth in the first step of the amorphization and the high Co concentration of the glass (on average). Homogenization of the alloy produces Kirkendall voids.

lishing a highly mobile crystalline-Co-Co-rich-glass interface. Note, that no Kirkendall voids are observed during this first step of the reaction, and it is of interest that the material can accommodate the stress involved in the diffusion process which might even help to form the amorphous phase.

If crystalline Zr is left after the first step of the reaction, homogenization of the system has to occur during a further step thus lowering the free energy of the system to its local minimum by reducing the Co content of the amorphous layer. Since we assume that Co atoms have a much higher diffusivity than Zr atoms in glassy Zr-Co alloys, the homogenization process will produce Kirkendall voids as shown in Fig. 2(c). The distance between the rows of these voids corresponds to the original thickness of the crystalline bilayer including the swelling, but the position is shifted to the middle of the original crystalline Co layer.

Growth of the amorphous layers seems to be diffusion-limited following a shifted  $\sqrt{t}$  law. To explore the kinetics of these reactions in more detail, systematic studies using cross-sectional transmission electron microscopy are currently under way.

The authors would like to thank C. R. M. Grovenor and K. N. Tu (IBM Thomas J. Watson Research Center, Yorktown Heights) for instructions on preparing cross-sectional TEM specimens. The financial help of the Deutsche Forschungsgemeinschaft (SFB 126E19 & Ko 668/3) is gratefully acknowledged.

<sup>1</sup>J. J. Hauser, *J. Phys. (Paris), Colloq.* **42**, C4-943 (1981).

<sup>2</sup>S. R. Herd, K. N. Tu, and K. Y. Ahn, *Appl. Phys. Lett.* **42**, 597 (1983).

<sup>3</sup>S. R. Herd, K. Y. Ahn, and K. N. Tu, *Thin Solid Films* **104**, 197 (1983).

<sup>4</sup>X. L. Yeh, K. Samwer, and W. L. Johnson, *Appl. Phys. Lett.* **42**, 242 (1983).

<sup>5</sup>K. Samwer, X. L. Yeh, and W. L. Johnson, *J. Non-Cryst. Solids* **61&62**, 631 (1984).

<sup>6</sup>R. B. Schwarz and W. L. Johnson, *Phys. Rev. Lett.* **51**, 415 (1983).

<sup>7</sup>R. B. Schwarz, K. L. Wong, W. L. Johnson, and B. M. Clemens, *J. Non-Cryst. Solids* **61&62**, 129 (1984).

<sup>8</sup>B. M. Clemens, W. L. Johnson, and R. B. Schwarz, *J. Non-Cryst. Solids* **61&62**, 817 (1984).

<sup>9</sup>M. van Rossum, M.-A. Nicolet, and W. L. Johnson, *Phys. Rev. B* **29**, 5498 (1984).

<sup>10</sup>W. L. Johnson, private communication.

<sup>11</sup>For example, see M. Natan, S. W. Duncan, and N. E. Byer, *J. Appl. Phys.* **55**, 1450 (1984).

<sup>12</sup>T. T. Sheng and R. B. Marcus, *J. Electrochem. Soc.* **127**, 737 (1980).

<sup>13</sup>K. Samwer, to be published.

<sup>14</sup>K. Samwer, A. Regenbrecht, and H. Schröder, in *Proceedings of the Fifth International Conference on Rapidly Quenched Metals, Würzburg, 1984* (to be published).

<sup>15</sup>L. Schulz, in *Proceedings of the Fifth International Conference on Rapidly Quenched Metals, Würzburg, 1984* (to be published).

<sup>16</sup>M. Atzmon, in *Proceedings of the Fifth International Conference on Rapidly Quenched Metals, Würzburg, 1984* (to be published).

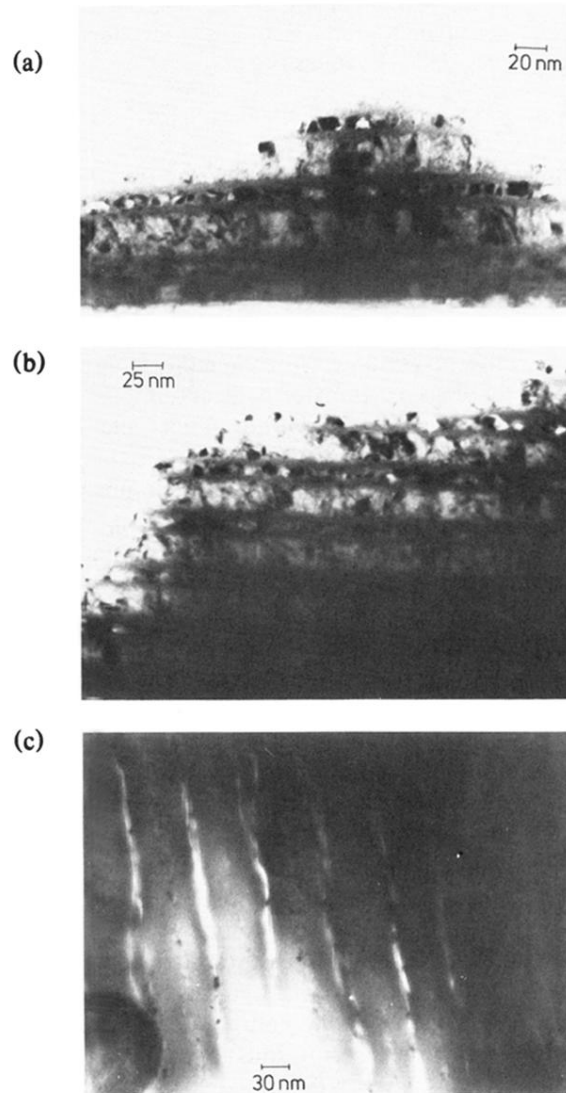


FIG. 2. (a) Cross-sectional TEM of a Zr-Co multilayer diffusion couple reacted 2 h at 210 °C (see text for explanation). (b) Same as (a) on a smaller magnification: Note the strictness of the glass formation at each interface and its planar growth. (c) Cross-sectional TEM of a Zr-Co multilayer diffusion couple reacted over 100 h at 210 °C. The reaction is almost complete with some remaining Zr crystals (black spots) and rows of Kirkendall voids.